East European Journal of Physics. 3. 280-285 (2026)
DOI:10.26565/2312-4334-2026-3-22 ISSN 2312-4334

A HIGH-SENSITIVITY, ZERO-BIAS SILICON PHOTODIODE FOR DETECTION OF ECO-FRIENDLY $AgInS_2$ та $CuInS_2$ QUANTUM DOT EMISSION

Mykola S. Kukurudziak[1,2*], Vasylyna V. Kopach[1], Serhii A. Voitovych[3], Yuriy B. Khalavka[1], Mykola S. Solodkyi[1]
[1]*Yuriy Fedkovych Chernivtsi National University, Kotsyubyns'kogo str. 2, 58012, Chernivtsi, Ukraine*
[2]*Rhythm Optoelectronics Shareholding Company, Holovna str. 244, 58032, Chernivtsi, Ukraine*
[3]*Ivano-Frankivsk National Medical University, Halytska str. 2, 76018, Ivano-Frankivsk, Ukraine*
**Corresponding Author e-mail: mykola.kukurudzyak@gmail.com*
Received May 24, 2026; revised July 23, 2026; accepted August 20, 2026

Silicon *p-n* photodiodes optimized for detecting a broad spectrum of photoluminescent radiation from $AgInS_2$ and $CuInS_2$ quantum dots have been developed and fabricated. By adjusting fabrication parameters and carefully selecting the substrate material, the sensor's spectral sensitivity peak (0.34 A/W) aligns with the nanocrystal emission range (550–700 nm). To maximize resolution, we operated the detector in zero-bias mode. This minimized dark current to approximately 6 pA, reduced thermal noise, and enabled high detection sensitivity. It has been experimentally established that, with a load resistance of 10 kΩ, the cutoff frequency of the photodiode is 1 MHz and is entirely limited by the RC time constant of the circuit. This frequency response is sufficient not only for steady-state radiometry of colloids and films with a radiation power of 0.29–0.35 mW, but also for precise study of the microsecond kinetics of quantum dot luminescence decay without risking photodegradation.
Keywords: *Quantum dots; $AgInS_2$; $CuInS_2$; Detector; Sensitivity; Photodiode*

A current trend in electronic sensor development is the use of various nanomaterials to miniaturize devices and enhance sensor sensitivity. The wide range of electronic, optical, and mechanical properties across different classes of nanomaterials opens up opportunities to develop sensors with unprecedented sensitivity, fast response, and reliability [1]. By principle of operation, most sensors developed today are electrical (resistive, capacitive, diode, electrochemical, or transistor type), while optical sensors (luminescent) are much less developed [2]. Existing optical and luminescent sensors use quantum dots (QDs), but are often based on toxic materials (Cd, Pb, etc.) [3,4], which limits their application in environmentally sensitive environments (e.g., water, bioenvironment). Therefore, interest is growing in "environmentally friendly" quantum dots—AgInS2 and CuInS2—that combine good optical/electronic properties with lower ecotoxicological risk [5-7]. The band gap of $AgInS_2$ varies between 1.8 and 2.2 eV, depending on the stoichiometric ratio of silver and indium during the synthesis of quantum dots. One of the key features of $AgInS_2$ is a broad emission band with a Stokes shift, mainly in the red-yellow region (550–750 nm). The band gap of $CuInS_2$ is approximately 1.45–1.55 eV. The main advantages of this material are high photosensitivity, good stability, and susceptibility to point-defect formation, particularly copper vacancies (V_{Cu}). Unlike linear defects, which usually degrade the spectroscopic and electrical properties of semiconductor structures [8], these intrinsic point defects positively affect photoluminescence (PL), significantly expanding the spectral range in which the material can operate. Using $AgInS_2$ and $CuInS_2$ nanoparticles, easy-to-use photoluminescence-based sensors with high selectivity, detection range, and sensitivity can be created [9].

The practical application of $AgInS_2$ and $CuInS_2$ nanoparticles in luminescent sensors is limited by detector sensitivity and the intensity of light emitted by these quantum dots. The intensity of the radiation in turn depends on several factors: intensity of the excitation diode; stability of the quantum dots; quantum yield of the nanoparticles; efficiency of absorption of the excitation light; spectral sensitivity of the detector. Thus, for optimal sensor performance based on these quantum dots, all these factors must be considered and balanced.

Our previously published experimental results [10] showed that the PL peak of AgInS2 nanocrystals (colloid) exhibits an emission from 700 nm (1.8 eV) to 575 nm (2.2 eV) with a change in the molar ratio of In/Ag precursors from 3 to 20. The PL spectrum of the layer-by-layer assembled $AgInS_2$ thin films (Fig. 1) are slightly shifted towards higher energy compared to the spectra of the original $AgInS_2$ solution and are in the range from 650 nm (1.9 eV) to 550 nm (2.3 eV). Despite the different shifts of the PL peak positions, the full width at half maximum (FWHM) of the PL spectra of the films are approximately the same for the corresponding colloids: 0.32-0.41 eV.

Increasing the irradiation intensity cannot be infinite, as it can cause photodegradation of quantum dots under real operating conditions. Therefore, the system design should be based on the detector's characteristics, which will determine whether to select nanoparticles with higher intensity. Such $AgInS_2$ and $CuInS_2$ quantum dot colloids can emit power around 0.29-0.35 mW that then require detection.

Cite as: M.S. Kukurudziak, V.V. Kopach, S.A. Voitovych, Y.B. Khalavka, M.S. Solodkyi, East Eur. J. Phys. 3, 280 (2026), https://doi.org/10.26565/2312-4334-2026-3-22

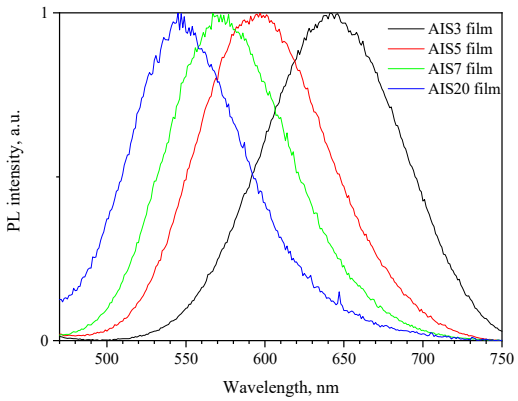

Figure 1. Photoluminescnece spectra of $AgInS_2$ QDs films; λ exc = 441.6 nm

Accordingly, developing quantum dot luminescence detectors is essential for the effective operation of the proposed systems. Undoubtedly, the use of photomultipliers [11] or avalanche photodiodes (PD) [12] could be effective; however, such detectors are expensive and complex to manufacture. One of the main advantages of the proposed system, in addition to its environmental friendliness, is the affordability and relative simplicity of manufacturing its components. Silicon *p-i-n* [13] and *p-n* [14] PDs can serve as an effective replacement for these photodetectors, as they possess sufficient sensitivity in the visible wavelength range that needs to be detected (λ = 550 nm, λ = 570 nm, λ = 590 nm, λ = 600 nm, λ = 650 nm). It is worth noting that *p-i-n* PDs are less suitable for the described purpose, since they typically operate at high reverse bias and have high sheet resistance and a long lifetime of minority carriers in the base, which, as is known, significantly shifts the peak of the photodiode's spectral sensitivity curve toward longer wavelengths up to λ = 1.02 μm [13, 15]. Furthermore, in *p-i-n* photodiodes, there is a need for high-concentration doping of the front region, which in turn absorbs a significant portion of the visible-range radiation; additionally, to mitigate surface generation, *p-i-n* photodiodes should be fabricated with guard ring systems, which subsequently requires the measurement and control of additional parameters [16]. These factors complicate the use of *p-i-n* photodiodes; therefore, it is proposed to use silicon *p-n* photodiodes for detecting visible luminescent radiation from $AgInS_2$ and $CuInS_2$ quantum dots. Accordingly, the aim of this work is to develop a silicon single-element *p-n* PD with enhanced detection sensitivity, which is planned to be achieved through the zero-bias mode, and to evaluate its performance during quantum dot irradiation simulations.

EXPERIMENTAL

The photodetectors were fabricated using *n*-type single-crystal dislocation-free FZ-Si with a [100] orientation and a resistivity of ρ ≈ 100–150 Ω·cm. The fabricated detectors are shown in Fig. 2. The area of the responsive element (RE) was A_{RE}=0.64 mm². The fabrication was carried out using planar diffusion technology.

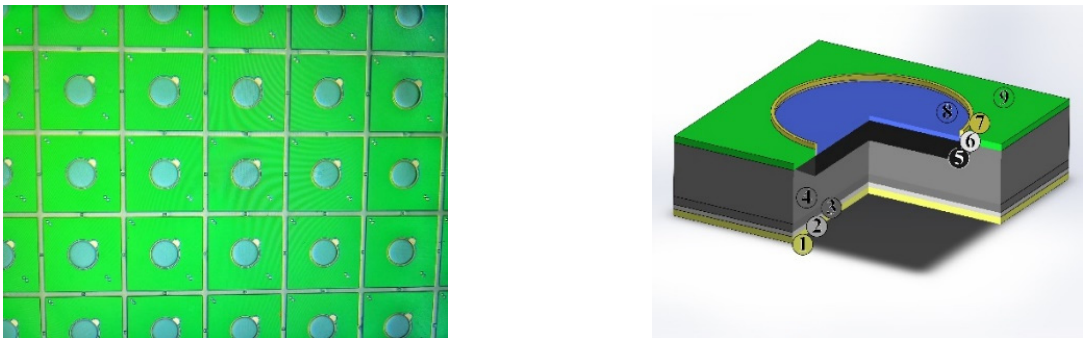

a b

Figure. 2. Image of photosensitive PD-crystals on a substrate (a) and three-dimensional view of the PD-crystal with a quarter cross-section illustrating (b): 1 — back-side Au-metallization, 2 — back-side Cr-sublayer, 3 — phosphorus-doped n^+-region, 4 — *n*-Si substrate, 5 — boron-doped p^+-RE, 6 — front-side Cr-sublayer, 7 — front-side Au-metallization, 8 — antireflection oxide layer of the RE; 9 — protective SiO_2

The photodiode fabrication process consisted of the following steps: oxidation of Si substrates in a hydrochloric acid vapor atmosphere at *T*=1403–1453 K; boron diffusion to form p^+-type photosensitive regions at 1273–1323 K, boron drive-in in an oxidizing atmosphere to form an anti-reflective coating and redistribute the dopant at temperatures of *T*=1403–1453 K, phosphorus diffusion toward the substrate at *T*=1203–1253 K to passivate generation-recombination centers within the photodiode crystal volume and form an ohmic n^+-layer; Cr-Au metallization and contact formation.

Given that visible radiation is absorbed in the near-surface layers of silicon [17], to ensure minimal recombination of photogenerated charge carriers in the n^+-layer, its thickness was approximately x_{p+-n}=1.5–2 μm. The anti-reflective coating was designed to satisfy the minimum reflection condition (1)[18], according to which for a wavelength of λ = 550 nm the oxide thickness is d_{SiO2}=96 nm, and for a wavelength of λ=650 nm it is d_{SiO2}=114 nm; accordingly, the SiO_2 thickness was selected to be approximately d_{SiO2}=100–110 nm.

$$\frac{\lambda}{4} = nd_{SiO_2} \quad (1)$$

where *n* is the refractive index of SiO_2.

Additionally, the method of forming a passivation coating in an atmosphere of hydrochloric acid vapor was selected for the manufacturing process, as this method minimizes the influence of uncontrolled impurities and contamination, particularly Na^+ and K^+ ions, and surface recombination [19, 20], which is particularly relevant for the design of devices without guard rings.

The dark current (I_d) and *I–V*-characteristics of PDs were measured using a hardware-software complex implemented on the basis of the Arduino platform, an Agilent 34410A digital multimeter and a Siglent SPD3303X programmable power source, which were controlled by a personal computer using software created by the authors in the LabView environment.

Monitoring of current monochromatic responsitivity ($S_{I\lambda}$) was carried out by method of comparing responsitivity of the investigated PD with a reference photodiode. Measurements were performed when illuminating the PD with a radiation flux of a power of not over P=2,5·10^{-5} W; load resistance across the responsive element R_l= 10 kΩ, at the reverse bias voltages of V = 0-15 V and modulation frequency f=1 kGz. The spectral characteristic of PD responsivity ($S(\lambda)$) at different bias was obtained out using the KSVU-23 automated spectral complex.

RESULTS OF THE RESEARCH AND THEIR DISCUSSION

From the dark *I-V* characteristics of the PD, it was established that its dark current increases with increasing reverse-bias voltage. The diffusion [21] and surface generation [16] components of the dark current can be considered constant and unchanging with increasing bias, while the volume generation component (I^G_d) increases due to the expansion of the space charge region (SCR) with increasing voltage (2) [21], so in this case, it can be assumed that the current of the fabricated photodiode is determined by the volume generation current. At 0 V, the dark current reaches 6 pF with a depletion-layer width of W_i = 3–4 μm (3) [22]. The dark current does not reach saturation within the voltage range studied because, at these voltages, its SCR does not saturate (Fig. 3).

$$I_d^G = e\frac{n_i}{2\tau}W_i A_{RE} \tag{2}$$

where n_i is own concentration of charge carriers in the substrate; e is the charge of the electron; τ is life time of minor charge carrier.

$$W_i = \left(\frac{2\varepsilon\varepsilon_0(\phi_c - U_{bias})}{eN_A}\right)^{\frac{1}{2}} \tag{3}$$

where ε, ε_0 are dielectric constants for silicon and vacuum, respectively; φ_c is contact potential difference.

It should also be noted that the base material used and the photodiode's operating mode allowed us to achieve the peak of the PD`s spectral response at λ_m≈650-670 nm (Fig. 4). This indicates that this wavelength is characterized by the most efficient collection of minority charge carriers in the silicon bulk, since according to the Beer–Lambert–Bouguer law [23], the intensity of light decreases by a factor of 2.72 at a depth of about 3–4 μm (absorption coefficient $\alpha \approx 2.5\cdot10^3$-$3\cdot10^3$ cm^{-1} [16]), and for light of this wavelength to be absorbed almost completely (by 95–99%), a silicon thickness of about 10–15 μm is required. Accordingly, it can be assumed that the effective diffusion length of holes in the PD base reaches about L_P=5–10 μm, which ensures the effective collection of photogenerated carriers in a silicon layer equal to W_i+L_p [24], since the quantum efficiency (QE) of the photodiode is determined by the probability of radiation absorption in this thickness (4).

$$QE(\lambda) \approx 1 - e^{-\alpha(\lambda)\cdot(W_i + L_n)} \tag{4}$$

We also obtained the dependencies of the photodiode's current monochromatic sensitivities at the wavelengths under study (Fig. 5).

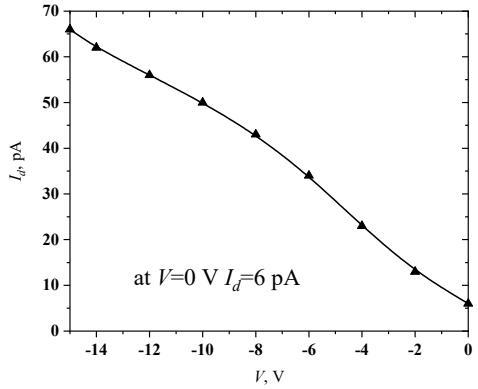

Figure 3. Dark *I-V* characteristic of the *p-n* PD

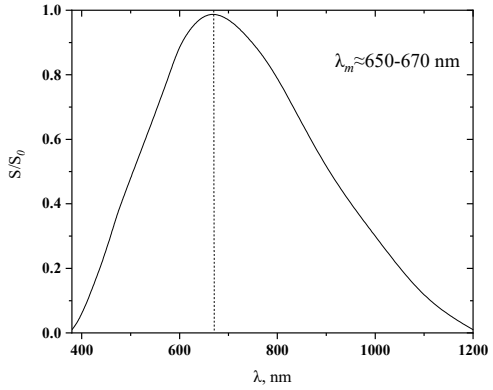

Figure 4. Relative spectral characteristic of the PD at V=0 V

Using these values, we determined the spectral characteristic of the quantum efficiency of the fabricated PD (Fig. 6) from the relationship between quantum efficiency and spectral sensitivity (5) [25]. It should be noted that in *p-n* PDs, as in the case under study, the photosensitivity is practically independent of voltage, since the effective collection region for photogenerated carriers increases minimally with an increase in reverse bias voltage due to the minimal resistivity, and the actual sensitivity of such PD is determined primarily by the diffusion length of the photogenerated charge carriers in the doped front zone and the base region.

Note, that the p^+-layer exhibits a gradual decrease in concentration as the depth of the p^+-n-junction increases; accordingly, the contribution of photogenerated charge carriers to the total sensitivity is significant. However, it should be noted that a significant amount of radiation is absorbed in the doped front p^+-region, so the PD`s *QE* in the visible range is less than 1 (Fig. 6).

$$S_\lambda = \frac{QE \cdot \lambda}{1.24} \tag{5}$$

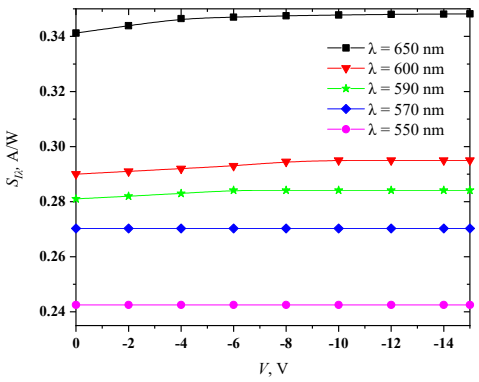

Figure 5. Dependence of the $S_{I\lambda}(V)$ of PDs

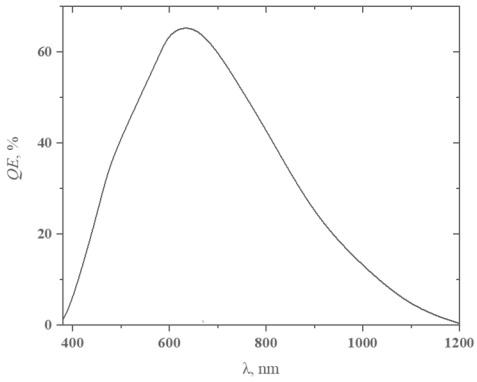

Figure 6. Spectral characteristic of the PD`s QE at V=0 V.

To evaluate the detection properties of the photodiodes, their specific detectivity (D^*) (6)[26] was determined. The fabricated photodiodes showed the highest detectivity at λ = 650 nm, since sensitivity is highest at this wavelength (Fig. 7). Furthermore, the detectivity decreases with increasing bias voltage due to the rise in dark current; however, at V = 0 V, the photodiodes exhibited a $D^* \approx 1.4$–2 cm·Hz$^{1/2}$ W^{-1}, which is a quite high value and can compete with analogues on the market.

$$D^* = \sqrt{\frac{A_{RE}}{2eI_d}} S_{I\lambda} \tag{6}$$

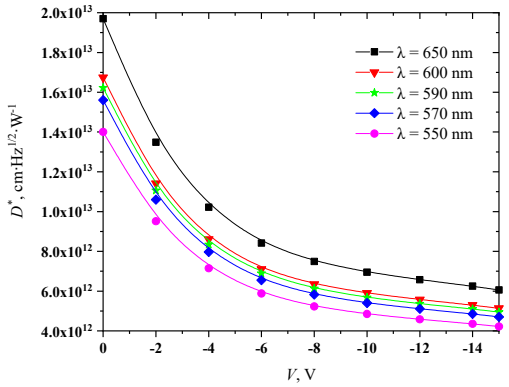

Figure 7. Dependence of the $D^*(V)$ of PDs

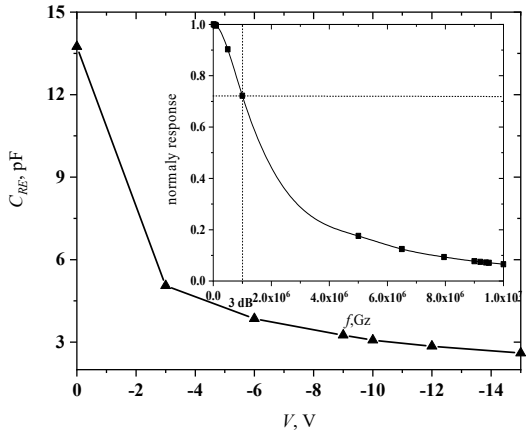

Figure 8. The *C-V* characteristic of a *p-n* photodiode and its amplitude-frequency response at 0 V (inset)

To evaluate the performance of the *p-n* photodiode, its *C-V* characteristics were investigated (Fig. 8). Based on the measured barrier capacitance, which is C_{RE} ≈14 pF at zero bias, the amplitude-frequency response of the sensor was calculated, taking into account a load resistance of 10 kΩ and a series base resistance of 150–200 Ω·cm. It was found that the cutoff frequency of the PD is 1MHz (τ_{RC}=150 ns) (Fig. 8 inset). Since the high value of the load resistance significantly exceeds the internal resistance of the base, the overall response of the structure in photogeneration mode without an external bias is entirely determined by the RC component of the circuit, while the contribution of the photon carrier transit time through the depleted region remains negligible.

The photodiodes produced can be used to measure a steady-state integral photocurrent. In addition to analyzing the steady-state spectral-energy characteristics, a crucial step in the comprehensive testing of the developed photodetector is the investigation of the photoluminescence decay kinetics of $AgInS_2$ and $CuInS_2$ quantum dots. Due to the dominant mechanism of donor-acceptor recombination, the lifetime of charge carriers in such triple nanostructures is abnormally long and typically lies in the microsecond range 100 ns — 1μs. Recording such relaxation processes in dynamic mode imposes stringent requirements on the response speed of the measurement circuit. Since the established cutoff frequency of the photodiode 1 MHz corresponds to a time constant of 150 ns, the developed system is capable of accurately recording long-duration kinetic decay curves, which opens up the prospect of its use in time-resolved photoluminescence spectroscopy.

Given that the PL spectra of the studied $AgInS_2$ nanocrystals cover a spectral range from 550 nm to 700 nm, depending on the In/Ag molar ratio (Fig. 1), an assessment of the photodetector's integral sensitivity for detecting this type of radiation was performed. By convolving the emission spectra of the QDs with the experimental curve of the PD`s relative spectral sensitivity at S_m = 0.34 A/W at a maximum of λ=650–670 nm, it was established that the device's integral sensitivity is 0.32 A/W for long-wavelength samples and gradually decreases to 0.26 A/W for short-wavelength samples. Since the output optical power of quantum dot luminescence is in the range of P=0.29–0. 35 mW, this level of integral sensitivity ensures the generation of a reliable photocurrent of ~75–110 μA, allowing for reliable signal detection without the risk of QDs photodegradation due to excessive excitation.

CONCLUSIONS

High-efficiency silicon *p-n* photodiodes have been developed with a spectral range optimized for detecting the luminescence of $AgInS_2$ and $CuInS_2$ quantum dots (550-700 nm). The detector's operation in zero-bias mode ensures a low dark current (~ 6 pA) and high system detectivity (1.4–2 cm·Hz$^{1/2}$ W^{-1}). With a response rate of 150 ns, the developed module is a reliable tool both for stationary radiometry of QDs emissions with power in the range of 0.29–0.35 mW, as well as for analyzing their microsecond decay kinetics.

Acknowledgments

This work was partially supported by the Ministry of Education and Science of Ukraine (grant number 0126U002507); YK is supported by MESU grant 0126U002293.

ORCID ID

Mykola S. Kukurudziak, https://orcid.org/0000-0002-0059-1387; **Vasylyna V. Kopach,** https://orcid.org/0009-0004-7927-983X
Serhii A. Voitovych, https://orcid.org/0000-0001-9141-808X; **Yuriy B. Khalavka,** https://orcid.org/0000-0002-6832-447X
Mykola S. Solodkyi, https://orcid.org/0000-0001-7432-9202

REFERENCES

[1] X. Sui, J.R. Downing, M.C. Hersam, and J. Chen, Materials Today, **48**, 135-154 (2021). https://doi.org/10.1016/j.mattod.2021.02.001
[2] Ya.O. Linevych, and V.M. Koval, Microsystems, Electronics and Acoustics, **27**(2), 264376–1 (2022). https://doi.org/10.20535/2523-4455.mea.264376
[3] E. Benavente, M. Alegría, P. Cortés, J. Aliaga, R. Villarroel, D. Guzmán, L. and Ballesteros, G., Journal of Environmental Chemical Engineering, **11** (3), 110025 (2023). https://doi.org/10.1016/j.jece.2023.110025
[4] Freeman, R., and Willner, I., Chem. Soc. Rev. **41**, 4067-4085 (2012). https://doi.org/10.1039/C2CS15357B
[5] X. Gao, X. Liu, Z. Lin, S. Liua, and X. Su. Analyst, **137**, 5620-5624 (2012). https://doi.org/10.1039/C2AN35888C
[6] A.S. Fuhr, H.J. Yun, N.S. Makarov, H. Li, H. McDaniel, and V.I. Klimov, ACS Photonics, **4**(10), 2425-2435 (2017). https://doi.org/10.1021/acsphotonics.7b00560
[7] Liu J., Zhao X., Xu H., Wang Z., and Dai Z. Anal Chem. **91**(14), 8987-8993 (2019). https://doi.org/10.1021/acs.analchem.9b01183
[8] I. Fodchuk, A. Kuzmin, O. Maslyanchuk, I. Hutsuliak, M. Solodkyi, Y. Roman, M. Solovan, and O. Gudymenko, Physics and Chemistry of Solid State, **23**(1), 114-149 (2022). https://doi.org/10.15330/pcss.23.1.144-149
[9] T. Xue, Y. Shi, J. Guo, M. Guo, and Y. Yan, Vacuum, **193**, 110514 (2021). https://doi.org/10.1016/j.vacuum.2021.110514
[10] V. Kopach, Y. Khalavka, Y. Yosypenko, N. Doskaliuk, O. Kopach, M. Dmytruk, I. Dmytruk, *et al*., Luminescence, **39**(10), e70001 (2024). https://doi.org/10.1002/bio.70001
[11] S.J. van der Sar, S.E. Brunner, and D.R. Schaart, Medical Physics, **48**(10), 6324-6338 (2021). https://doi.org/10.1002/mp.14886
[12] J. Jegal, H.W. Park, and H.J. Kim, IEEE Transactions on Nuclear Science, **68**(6), 1304-1308 (2021). https://doi.org/10.1109/TNS.2021.3070040
[13] M.S. Kukurudziak, E.V. Maistruk, R. Yatskiv, I.P. Koziarskyi, and D. P. Koziarskyi, Journal of Physics D: Applied Physics, **58**(16), 165106 (2025). https://doi.org/10.1088/1361-6463/adbd4d
[14] V.G. Verbitskiy, V.S. Antonyuk, A.O. Voronko, L.M. Korolevych, D.V. Verbitskiy, and D.O. Novikov, Journal of Nano- and Electronic Physics, **13**(4), 1-6 (2021). https://doi.org/10.21272/jnep.13(4).04029
[15] A. Voronko, D. Novikov, and O. Shymanovskyi, Radioelectronics and Communications Systems, **66**(2), 74-84 (2023). https://doi.org/10.3103/S073527272302005X
[16] M.S. Kukurudziak, Journal of Instrumentation, **19**(09), P09006 (2024). https://doi.org/10.1088/1748-0221/19/09/P09006
[17] S.M. Sze, and K.K. Ng, *Physics of semiconductor devices*, (Wiley, 2006).
[18] S.B. Khan, S. Irfan, Z. Zhuanghao, and S.L. Lee, Materials, **12**(9), 1483 (2019). https://doi.org/10.3390/ma12091483

[19] H. B. Zhang, W. Q. Li, and D. W. Wu, J. Electron Microsc. **58**(1), 15–19 (2009). https://doi.org/10.1093/jmicro/dfn024
[20] N. Akchurin, G. Altopp, B. Burkle, W.D. Frey, U. Heintz, N. Hinton, M. Hoeferkamp, *et al*., Journal of Instrumentation, **18**, P08001 (2023). https://doi.org/10.1088/1748-0221/18/08/P08001
[21] K.V. Ravi, *Imperfections and impurities in semiconductor silicon*, (Wiley, New York, 1981).
[22] A.V. Fedorenko, Technology and design in electronic equipment, **17**(3–4), 17 (2020). https://doi.org/10.15222/TKEA2020.3
[23] A.V. Igo, Opt. Spectrosc. **128**, 1125 (2020). https://doi.org/10.1134/S0030400X20080135
[24] M.S. Kukurudziak, and E.V. Maistruk, East Eur. J. Phys. **1**, 386 (2024). https://doi.org/10.26565/2312-4334-2024-1-39
[25] F. Alghannam, N.S. Alharthi, & M. Alayed, Frontiers in Physics, **13**, 1563838 (2025). https://doi.org/10.3389/fphy.2025.1563838
[26] S.N. Moger, and M. Mahesha, Sensors and Actuators A: Physical, **315**, 112294 (2020). https://doi.org/10.1016/j.sna.2020.112294

ВИСОКОЧУТЛИВИЙ КРЕМНІЄВИЙ ФОТОДІОД ІЗ НУЛЬОВИМ ЗМІЩЕННЯМ ДЛЯ ВИЯВЛЕННЯ ВИПРОМІНЮВАННЯ ЕКОЛОГІЧНО БЕЗПЕЧНИХ КВАНТОВИХ ТОЧОК $AgInS_2$ ТА $CuInS_2$ †

Микола С. Кукурудзяк[1,2], Василина В. Копач[1], Сергій А. Войтович[3], Юрій Б. Халавка[1], Микола С. Солодкий[1]
[1]Чернівецький національний університет імені Юрія Федьковича, 58002, м. Чернівці, вул. Коцюбинського, 2, Україна
[2]АТ «Центральне конструкторське бюро Ритм», 58032, м. Чернівці, вул. Головна, 244, Україна
[3]Івано-Франківський національний медичний університет, 76018, м. Івано-Франківськ, вул. Галицька, 2, Україна

Розроблено та виготовлено кремнієві *p-n* фотодіоди, оптимізовані для детектування широкого спектра фотолюмінесцентного випромінювання квантових точок $AgInS_2$ та $CuInS_2$. Завдяки коригуванню технологічних режимів виготовлення структури та прецизійному вибору базового матеріалу, максимум спектральної чутливості сенсора (0.34 А/Вт) повністю узгоджено з діапазоном емісії нанокристалів (550-700 нм). Для забезпечення максимальної роздільної здатності визначено роботу детектора в режимі нульового зміщення. Це дозволило мінімізувати темновий струм до значення близько 6 пА, зменшити теплові шуми й досягти високої детективності вимірювальної системи. Експериментально встановлено, що за опору навантаження 10 кОм гранична частота фотодіода становить 1МГц і повністю лімітується *RC*-постійною кола. Такий частотний відгук є цілком достатнім не лише для стаціонарної радіометрії колоїдів і плівок із потужністю випромінювання 0.29-0.35 мВт, а й для точного дослідження мікросекундної кінетики затухання люмінесценції квантових точок без ризику їхньої фотодеградації.

Ключові слова: *квантові точки; $AgInS_2$; $CuInS_2$; детектор; чутливість; фотодіод*